JOURNAL OF CATALYSIS **171,** 279–286 (1997)
ARTICLE NO. CA971792

The State of Zirconia Supported Platinum Catalysts for CO_2/CH_4 Reforming

J. H. Bitter, K. Seshan, and J. A. Lercher[1]

Faculty of Chemical Technology, Catalytic Processes and Materials, University of Twente, P.O. Box 217, 7500 AE, Enschede, The Netherlands

Received November 18, 1996; revised June 5, 1997; accepted June 16, 1997

In Pt/ZrO_2 catalysts used for CO_2/CH_4 reforming to syngas, not all accessible Pt contributes equally to the activity of the catalyst. The catalytic activity is determined by the accessibility of Pt on the Pt-ZrO_2 perimeter. This is explained in terms of the CO_2 activation via carbonate species on the support which must be in the proximity of the Pt particles to react with the methane activated on the metal. The significance of the support is also emphasized by the low activity of Pt black and Pt/SiO_2, which were incapable of forming carbonates on the support. The perimeter concentration of Pt/ZrO_2 can be changed by changing the Pt concentration in the catalyst or by increasing the calcination temperature which causes sintering of the Pt particles. In contrast to the calcination temperature, the reduction temperature did not influence the activity although the hydrogen chemisorption capacity was markedly decreased by increasing the reduction temperature. As sintering was excluded on basis of particle size determination from EXAFS results a SMSI state on Pt/ZrO_2 during high temperature reduction is concluded to exist. This state does not persist under reaction conditions due to the presence of adsorbed oxygen from CO_2 dissociation.

INTRODUCTION

Carbon dioxide reforming of methane to produce synthesis gas, i.e., a mixture of carbon monoxide and hydrogen ($CO_2 + CH_4 \quad 2CO + 2H_2$; $\Delta H^\circ_{298\,K} = 247.0$ kJ/mol) has attracted substantial interest (1–4). The reaction is well suited to produce CO rich synthesis gas or very pure carbon monoxide for the synthesis of bulk chemicals such as acetic acid, dimethyl ether, and alcohols via the oxoalcohol synthesis (5). More significantly, for acetic acid manufacture carbon dioxide reforming is estimated to have economic advantages over other synthesis gas production routes (6). However, the feasibility of CO_2 reforming depends strongly on the price and availability of CO_2 and the pressure at which the process will be operated.

The reaction consists of similar elementary reaction steps as steam reforming ($H_2O + CH_4 \quad CO + 3H_2$; $\Delta H^\circ_{298\,K} =$ 206 kJ/mol) (7), but the absence of water and the high C/H ratio in the reactant feed favours extensive coke formation (8). Minimization of coking rates is, thus, one of the key aspects for designing a stable catalyst for the reaction. Coke forms readily via methane decomposition ($CH_4 \rightleftarrows C + 2H_2$; $\Delta H^\circ_{298\,K} = +74.9$ kJ/mol) and CO disproportionation ($2CO \rightleftarrows C + CO_2$; $\Delta H^\circ_{298\,K} = -172.4$ kJ/mol). Options to reduce the coke build up are (i) the addition of water (coupling with steam reforming), (ii) the addition of oxygen (coupling with partial oxidation), or (iii) the use of catalysts which minimize the rate of coking.

As early as 1928, Fischer and Tropsch showed that different metals have different activities for CO_2/CH_4 reforming and that most group VIII metals show appreciable activity for CO_2/CH_4 reforming (9). Many authors have investigated different metals like Ni, Ru, Rh, Pt, Ir, Pd (1, 10–13) for the reaction. Although there is some debate about the order of activity of these metals, Rh was preferred by most authors due to the good activity and stability for the catalyst. Ni catalysts, however, are commercially more interesting compared to noble metals but their main drawback is the high rate of coke formation (2, 12, 14, 15). From an economic point of view (relatively low price and good availability) Pt is a reasonable compromise.

The most commonly used support for CO_2/CH_4 reforming is Al_2O_3 (2, 9, 12, 16–18). Modifications to the support were sometimes made (9, 18, 19) by addition of basic promoters such as MgO and CaO to enhance catalyst stability. This indicates the importance of the support on the stability of the catalyst. Indeed a significant influence of the support is observed for Pt catalysts and we have shown earlier that ZrO_2 is a very well suited support (20–23).

In order to grasp why Pt/ZrO_2 is a stable and active catalyst it is necessary to understand the nature of Pt in this catalyst, its interaction with the support and the contribution of ZrO_2 to the reaction and the elementary reaction steps that occur. In the present contribution the physical characteristics of the catalyst and their influence on catalytic behaviour is discussed.

METHODS

Catalyst Preparation

All catalysts used in this study were prepared by the wet impregnation technique. For this purpose a solution

[1] E-mail: J.A.Lercher@utct.ct.utwente.nl.

0021-9517/97 $25.00

of $H_2PtCl_6 \cdot 6H_2O$ in water (0.01 g Pt per ml) was used. The chosen support was first calcined for 15 h at 1125 K (heating rate 3 K/min) in flowing air (30 ml/min (NTP)). The support was then isostatically pressed into pellets at 4000 bars for 5 min. The pellets were crushed and sieved to give grains having diameters between 0.3 and 0.6 mm. The grains were impregnated with the H_2PtCl_6 solution to yield a catalyst with 0.5 wt% Pt. The catalysts were dried at 365 K for 2 h in a rotating evaporator followed by drying over night at 395 K in static air. Subsequently, the impregnated grains were calcined at 925 K for 15 h (heating rate 3 K/min). The Pt content of the catalyst was determined by atomic absorption spectroscopy. The following supports were used: γ-Al_2O_3 (000-3AQ, AKZO), TiO_2 (P-25, Degussa, mixture of anatase and rutile), SiO_2 (AKZO, F7), and ZrO_2 (RC-100, Gimex, monoclinic). The supports had the following surface areas, after calcination at 1125 K for 15 h: γ-Al_2O_3, 110 m^2/g; TiO_2, 7 m^2/g; SiO_2, 220 m^2/g; ZrO_2, 18 m^2/g.

Catalyst Characterizations

Hydrogen chemisorption measurements. Hydrogen chemisorption was carried out in a volumetric system. The sample (usually 1.5 g) was reduced for 2 h at 673 K in H_2 (when a higher reduction temperature was required, the sample was previously reduced *ex situ* at the higher temperature). After reduction the sample was degassed at 673 K for 1 h in high vacuum (10^{-6} mbar). The sample was cooled to room temperature (295 K) and the H_2 adsorption isotherm was measured by feeding decreasing amounts of H_2 (in the range 500–0 mbar) to the sample. The hydrogen chemisorption capacity was calculated by extrapolation of the hydrogen uptake to zero pressure.

The length of the Pt-ZrO_2 perimeter was calculated from hydrogen chemisorption values (H/Pt). From the H/Pt ratios particle sizes could be calculated using data published by Kip *et al.* (24) and Vaarkamp *et al.* (25). The same models were used to calculate metal dispersion based on the hydrogen chemisorption capacity. The H/Pt stoichiometry increases with decreasing particle size because smaller particles have a higher concentration of edges and corners, where more than one hydrogen atom per metal atom can adsorb, than larger particles (24, 25). Thus, by using these models varying H/Pt ratios were used for calculation the Pt dispersion.

XAS measurements. XAS measurements were performed at the Synchrotron facility in Daresbury (beamline 9.2). The catalyst powder was pressed into a self-supporting wafer (110 mg for Pt/ZrO_2 and 300 mg for Pt/γ-Al_2O_3, both catalysts contained 1 wt% Pt). The catalysts were *ex situ* reduced at the desired temperature. Prior to the EXAFS experiments catalysts were rereduced *in situ* at 675 K. EXAFS measurements were carried out at liquid nitrogen temperature. To isolate the EXAFS from the X-ray absorption edge, a polynomial function characteristic of the background was subtracted. The oscillations were normalized by the mass areal loading of the metal. The oscillations were k^2-weighted and Fourier transformed within the limits $k = 3.5$ to $k = 18$ to isolate the contributions of the different coordination shells.

IR spectroscopic measurement of CO_2 adsorption on Pt/ZrO_2. The catalyst powder was pressed into a self-supporting wafer. This wafer was analyzed *in situ* during the reaction by means of transmission absorption IR spectroscopy using a Bruker IFS 88 FTIR spectrometer (resolution 4 cm^{-1}). The IR cell was constructed as a continuously stirred tank reactor (volume 1.5 cm^3) equipped with $\frac{1}{16}$-in. gas in- and outlet tubing and CaF_2 windows. The partial pressure of each of the reactants (CO_2 and CH_4) was 250 mbar, the difference to 1 bar being He.

Catalyst testing. Typically 300 mg of catalyst were loaded into a tubular quartz reactor (inner diameter 5 mm) which was placed in an oven. The catalyst grains were kept in place by quartz wool plugs. A thermocouple was placed on top of the catalyst bed to measure the catalyst temperature. The oven temperature was controlled by a Eurotherm temperature controller. The catalysts were reduced *in situ* with 5% H_2 in N_2 for 1 h at 1125 K. After reduction the temperature was lowered in Ar to the (initial) reaction temperature and the feed gas mixture (25% CH_4 (vol), 25% CO_2, 5% N_2, and 45% Ar for a total flow of 170 ml $\cdot$ min^{-1}) was switched to the reactor. The reaction products were analysed in a gas chromatograph (Varian 3300), equipped with two 3-m carbosieve columns and a TCD.

RESULTS

Influence of the Fraction of Accessible Pt

Previous work from our group showed that 1 wt% Pt/ZrO_2 was an excellent catalyst for CO_2/CH_4 reforming in (20–23). It operated for 500 h without significant deactivation. In Fig. 1 the activity of 0.5 and 1 wt% Pt/ZrO_2 at 875 K are shown. The physico-chemical characteristics of these catalysts are compiled in Table 1. Note that both catalysts showed allmost the same activity although the 1 wt% catalyst exposed more Pt atoms compared to the 0.5 wt% catalyst (Table 1).

Figure 2 displays the variation of the catalytic activity at 875 K and the accessible Pt concentration for the series of Pt/ZrO_2 catalysts with different Pt loadings. With increasing metal loading the concentration of accessible Pt increased. However, while at a low Pt content (<0.5 wt%) the activity increased with increasing metal loading, the increase in activity stagnated at higher metal loading (>0.5 wt%). This could not be due to blocking of the pores by Pt because adsorption/desorption studies showed that the average pore

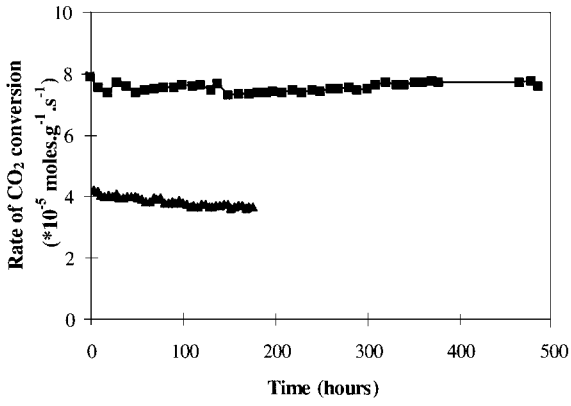

FIG. 1. Activity of 0.5 and 1 wt% Pt/ZrO_2 catalysts for CO_2/CH_4 reforming at 900 K, $CO_2/CH_4/He/N_2 = 42/42/75/10$, 300 mg catalyst, ■ = 1 wt% Pt/ZrO_2 (*2), ▲ = 0.5 wt% Pt/ZrO_2.

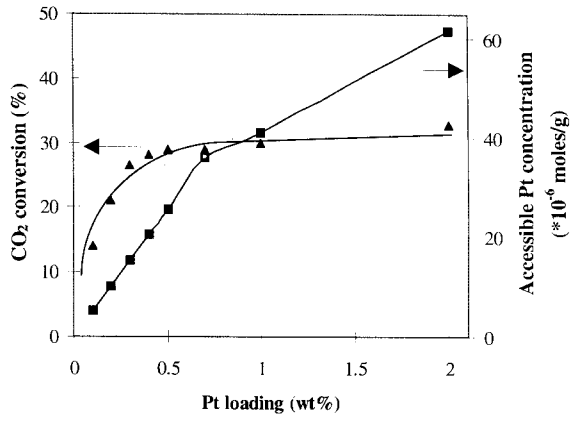

FIG. 2. Influence of the Pt-loading on the amount of accessible Pt and the activity of Pt/ZrO_2 catalysts for CO_2/CH_4 reforming at 875 K, $CO_2/CH_4/He/N_2 = 42/42/75/10$, 300 mg catalyst.

size is 28 nm and cylindrical in shape, whereas the largest Pt particle size is 2 nm (Table 1). Using catalysts with different grain sizes (0.1–1.0 mm in fractions of 0.1 mm) revealed that the CO_2 conversion was independent of the grain size, thus, internal mass transfer limitations were ruled out. Also external mass transfer limitations could be ruled out since the use of varying amounts of catalyst (200–600 mg catalyst) and keeping the contact time constant, i.e., at constant W/F (W = catalyst mass, F = total gas flow) did not show an influence on the conversion. In the above experiment, changing the gas flow, at constant contact time, changes the amount of heat that could be transferred from the gas phase. Since this and the fact that changing the diluent (He or Ar) did not influence the activity it is concluded that heat transfer limitations were absent. Thermodynamic limitations were also ruled out since the carbon dioxide conversion calculated from thermodynamics is 55% at 875 K, whereas the maximum conversion observed under the experimental conditions is 33% (Fig. 2). It is therefore concluded that the nonlinear dependence for the activity of Pt/ZrO_2 as a function of the accessible Pt area is a result of a change in the catalytic properties at higher metal concentrations.

The activity of Pt catalysts for CO_2/CH_4 reforming per accessible Pt atom is a compiled in Table 2. The unsupported Pt black catalyst was prepared as described by Paal *et al.* (26) using the "hydrazine method." After reduction of the catalyst at 975 K its surface area was 0.25 m^2/g (measured by the BET method and calculated from hydrogen chemisorption). From Table 2 it can be seen that the catalytic activity of Pt-black (TOF) is two orders of magnitude lower compared to Pt/ZrO_2, Pt/TiO_2, and $Pt/\gamma\text{-}Al_2O_3$. The activity of Pt-black compares, however, well with the low activity of Pt/SiO_2. This leads to the conclusion that the use of a suitable support can strongly increase the activity of the Pt metal. The positive involvement of the support for the reaction was shown by the use of Pt-black impregnated with a solution of $ZrOCl_2$ (and subsequent calcination and reduction at 875 K). The activity per accessible Pt atom of this catalyst was increased by an order of magnitude compared to the untreated Pt-black sample. The increase in activity of Pt-black after impregnation with $ZrOCl_2$ indicates

TABLE 1

Physico-Chemical Characteristics of Pt/ZrO_2 Catalysts with Different Metal Loadings

Pt loading (wt%)	Hydrogen chemisorption capacity (H/M)	Pt dispersion[a] (%)	Pt particle size[a] (nm)	BET surface area (m^2/g)
0.2	1.35 ± 0.1	100	0.8	18
0.3	1.30 ± 0.1	100	0.8	20
0.4	1.25 ± 0.1	100	0.9	19
0.5	1.10 ± 0.1	100	1.0	18
0.7	1.01 ± 0.1	97	1.2	18
1.0	0.82 ± 0.1	80	1.3	17
2.0	0.61 ± 0.1	58	1.9	20

[a] Calculated from hydrogen chemisorption as described by Kip *et al.* (24).

TABLE 2

Comparison of the Activities of Different Pt-Catalysts (0.5 wt% Pt/Support), $T = 925$ K, $CO_2/CH_4/He + N_2 = 50/50/50100$ ml · min^{-1}

Catalyst	Pt surface area (m^2/g)	TOF of CO_2 (s^{-1})
Pt/ZrO_2	1.2	20
$Pt/\gamma\text{-}Al_2O_3$	0.96	25
Pt/TiO_2	0.31	52
Pt/SiO_2	0.15	0.2
Pt-black	0.25	0.1
Pt-black/ZrO_2	0.24	1.1

TABLE 3

Influence of the Calcination Temperature on Activity, Hydrogen Chemisorption Capacity, and Pt Coordination Number of Pt/ZrO_2

Metal loading (wt%)	Calcination temperature[a] (K)	Coordination number from EXAFS[b]	Hydrogen chemisorption capacity[c] (H/Pt)	CO_2 conversion at 875 K (%)
1	925	6.5 (86)	0.82 (80)	30
1	1125	10.7 (20)	0.33 (33)	8
0.5	925	—	1.1 (100)	29
0.5	1025	—	0.50 (48)	24
0.5	1125	—	0.35 (33)	7

[a] To avoid a SMSI state (see Discussion) the catalysts were reduced at 775 K.

[b] Number between brackets denotes the Pt dispersion (%) as calculated from the coordination number (24).

[c] Number between brackets denotes the Pt dispersion (%) as calculated from the H/Pt ratio (24).

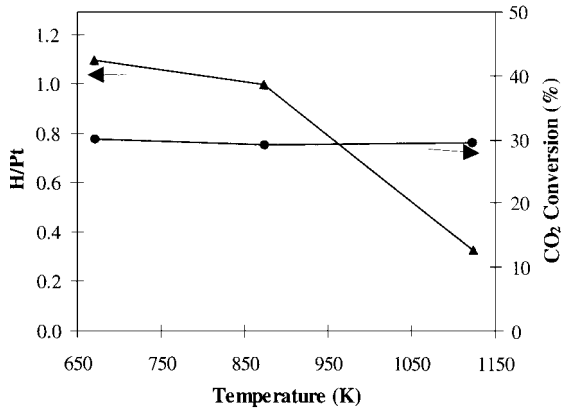

FIG. 3. Influence of the reduction temperature of Pt/ZrO_2 on the hydrogen chemisorption capacity and activity of the catalyst.

clearly that ZrO_2 contributes to the activity of Pt/ZrO_2 for the reforming reaction.

Influence of Pretreatment Procedure

Although Pt/ZrO_2 is a stable and active catalyst for CO_2/CH_4 reforming, the catalyst is sensitive to the preparation procedure, in particular the calcination temperature. The preparation of the catalyst involved calcination of the support grains, followed by impregnation of the grains with a H_2PtCl_6 solution. This catalyst precursor was calcined prior to *in situ* reduction and testing. The temperature of calcination of the blank support did not influence the activity of the catalyst, although the surface area (BET) decreased from 33 to 18 m^2/g when the calcination temperature was increased from 925 to 1125 K. On the other hand, the calcination temperature after impregnation had a significant influence on the activity of the catalyst due to Pt metal area loss. This can be seen from the EXAFS data from this sample, which showed an increase in coordination number from 6.5 to 10.7 when the calcination temperature was increased from 925 to 1125 K (Table 3). These results were confirmed by hydrogen chemisorption measurements which showed a decrease of H/Pt ratio from 0.82 to 0.33 as the calcination temperature was increased. Consequently, increasing the calcination temperature of the catalyst caused therefore a significant drop in activity (Table 3).

The temperature of *in situ* reduction, prior to testing of the catalyst, did not influence the activity of the Pt/ZrO_2 catalyst (Fig. 3). However, with increasing reduction temperature (from 675 to 1125 K) the hydrogen chemisorption capacity of the catalysts decreased significantly (the H/Pt ratio decreased from 1.1 to 0.33; Fig. 3), indicating sintering. EXAFS measurements, on the other hand, showed that the Pt coordination number and, thus, the Pt particle size did not increase (Table 4). The values for the percentage of metal exposed obtained by hydrogen chemisorption for samples that were reduced at low temperature (775 K) and by EXAFS are in good agreement. When a Pt/ZrO_2 catalyst with an apparent low dispersion (H/Pt = 0.33, reduction temperature 1125 K) was treated with 0.1% O_2 or air a higher dispersion (H/Pt = 0.7) was obtained (Table 4). This

TABLE 4

Influence of the Reduction Temperature on Activity, Hydrogen Chemisorption Capacity, and Pt Coordination Number of Pt/ZrO_2

Catalyst	Reduction temperature (K)	Coordination number from EXAFS	Dispersion from EXAFS (%)	H/Pt[b]	CO_2 conversion at 875 K (%)
1 wt% Pt/ZrO_2	775	6.5	86	0.82 (80)	30
1 wt% Pt/ZrO_2	1125	7.0	81	0.33 (33)	29
0.5 wt% Pt/ZrO_2	775	—	—	1.1 (100)	29
0.5 wt% Pt/ZrO_2	1125	—	—	0.35 (33)	28
0.5 wt% Pt/ZrO_2	1125/875/675[a]	—	—	0.70 (67)	28

[a] First temperature (1125 K) is the initial reduction temperature; second temperature is the oxidation temperature; third temperature is the reduction temperature before chemisorption measurement.

[b] Number between brackets denotes the Pt dispersion (%) as calculated from the H/Pt ratio (24).

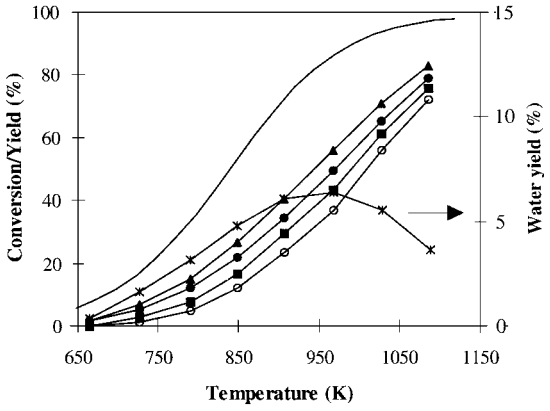

FIG. 4. Activity of 0.5 wt% Pt/ZrO_2, 300 mg catalyst, total flow = 170 ml · min^{-1}, $CO_2/CH_4/N_2 + He = 1/1/2$ (▲ = CO_2, ● = CO, ■ = CH_4, ○ = H_2, ∗ = H_2O, — = CO_2 thermodynamic conversion).

indicates that part of the metal area is lost due to covering with (presumably partially reduced) ZrO_2 (a SMSI type state) (28, 29).

The activity of 0.5 wt% Pt/ZrO_2 as function of temperature is plotted in Fig. 4. For comparison, the conversions and yields as predicted by thermodynamics are shown in Fig. 5. Under the chosen reaction conditions Pt/ZrO_2 did not reach thermodynamic conversions. It can be seen from Fig. 5 that, in addition to H_2 and CO, a significant amount of water was also produced. The water yield showed a maximum at 950 K. The H_2/CO ratio was always smaller than 1 and tended to 1 only at higher temperatures. The methane conversion was always lower than the CO_2 conversion, although they were present in the feed in a 1 : 1 ratio.

DISCUSSION

Figure 1 demonstrates clearly that both 0.5 and 1 wt% Pt/ZrO_2 are stable catalysts for CO_2/CH_4 reforming. It is, however, remarkable that both catalysts showed similar activities for the reforming reaction, while the former catalyst has a lower amount of exposed Pt compared to the latter (Table 1). As can be seen in Fig. 2 there is no simple relation between accessible Pt area and the activity of the catalyst. For catalysts with Pt contents above 0.5 wt% the amount of accessible Pt still increases, whereas the activity of the catalyst remains almost constant. Pore blocking, heat and mass transfer, as well as thermodynamic limitations, were ruled out by appropriate experiments (see results). It is thus concluded that not all accessible Pt contributes equally to the activity of the catalyst. When the activity of the catalyst was plotted as function of the Pt concentration on the Pt-ZrO_2 perimeter a linear dependence is observed (Fig. 6). The lengths of the different perimeters obtained for Pt/ZrO_2 catalysts with different metal loadings are represented by the diamonds (◆). Alternatively, the perimeter length was varied by changing the calcination temperature of the 0.5 wt% Pt/ZrO_2 catalyst. Increasing the calcination temperature (925, 1025, 1125 K) decreased the dispersion of this catalyst due to sintering (Table 3) which resulted in a decrease of the concentration of the Pt-ZrO_2 perimeter. These three points (calcination temperature = 925, 1025, and 1125 K) are also shown in Fig. 6 and represented by the asterisks (∗). These points also fit very well the line in the figure which describes the linear relation between the Pt perimeter and activity for the catalyst. This also indicates that the higher calcination temperature changed the perimeter concentration, but does not change the nature of the active sites.

The linear relation between the amount of Pt on the perimeter and the activity can either imply that the reaction takes place on the Pt-ZrO_2 perimeter or that the migration of a species formed on the support to the metal is rate determining in the reaction. When ZrO_2 was impregnated on Pt-black the activity of Pt-black was increased by an order

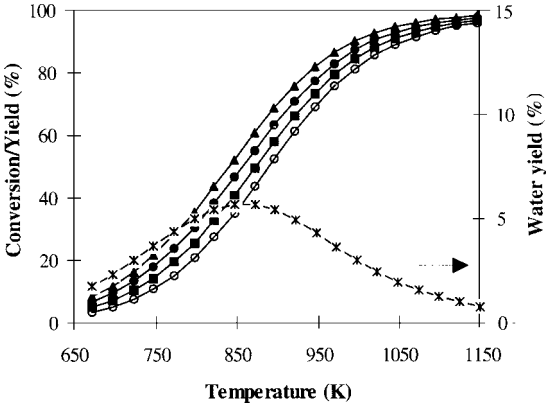

FIG. 5. Equilibrium conversions and yield as predicted by thermodynamics for a $CO_2/CH_4/He$ = 1/1/2 mixture (▲ = CO_2, ● = CO, ■ = CH_4, ○ = H_2, ∗ = H_2O).

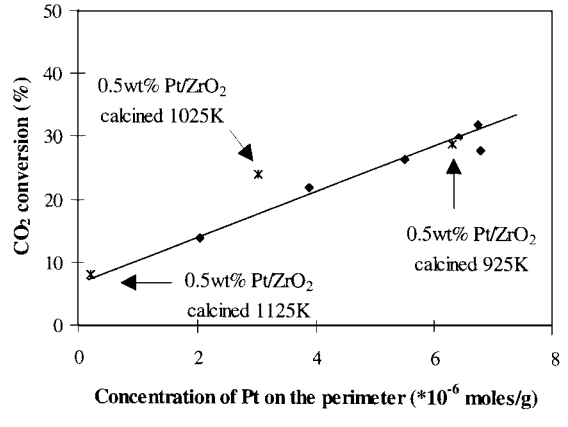

FIG. 6. Influence of the amount of accessible Pt on the activity of Pt/ZrO_2 catalysts for CO_2/CH_4 reforming at 875 K. ◆ = Pt/ZrO_2, ∗ = 0.5 Pt/ZrO_2 calcined at different temperatures.

of magnitude. This clearly shows that although Pt alone is active for CO_2/CH_4 reforming the activity can be significantly enhanced by the presence of a support. The enhancement of catalyst activity by the support was also shown for different other reactions. Levin *et al.* (30, 31) observed for CO_2/CO methanation an increase in the activity of Rh when it was decorated by partially reduced titania. Similar observations were made by Boffa *et al.* using oxides like NbO_x, TaO_x, and ZrO_x (32). Koerts *et al.* Observed a decrease of the activation energy for CO methanation over Rh/SiO_2 when the catalyst was doped with vanadium indicating the significance of the support for this reaction (33). The involvement of the support in the reaction mechanism was also shown for the watergas-shift reaction ($CO + H_2O \quad H_2 + CO_2$). A mechanism involving the formation of formates on the support, their migration to the metal, followed by decomposition on the metal was discussed (34). The importance of the support for the reforming reaction is also substantiated by the use of Pt-black which is at least two orders of magnitude less active, compared to Pt/ZrO_2 (Table 2).

Having established that the perimeter is decisive for dry methane reforming, the remaining question to be addressed is the role of the support on a molecular level. Infrared spectroscopic studies of CO_2 adsorption on Pt-catalysts showed the formation of linearly bound CO on Pt, and carbonate type species on the support for $Pt/\gamma\text{-}Al_2O_3$, Pt/TiO_2, and Pt/ZrO_2 (Fig. 7), although the type of carbonate species seems to be different for the various supports. Pt/SiO_2 did not show the formation of carbonate type species on the support while it proved to be active for methane decomposition. On Pt-black no carbonates could be formed on the support because this catalyst is unsupported. In general, it can be concluded that the catalysts which could form carbonates on the support ($Pt/\gamma\text{-}Al_2O_3$, Pt/TiO_2, Pt/ZrO_2, and Pt-black/ZrO_2; see Table 2) showed a much higher activity compared to the catalysts which could not form carbonates on the support (Pt-black, Pt/SiO_2). Note in this context

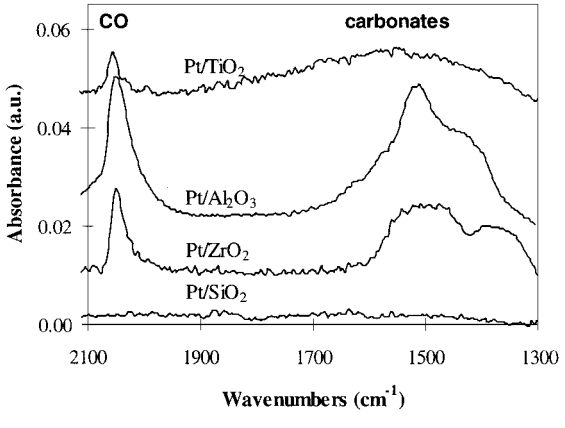

FIG. 7. Infrared spectra of CO_2 adsorption on different Pt catalysts, $T = 775$ K, $pCO_2 = 0.25$, total flow $= 30$ ml $\cdot$ min^{-1}.

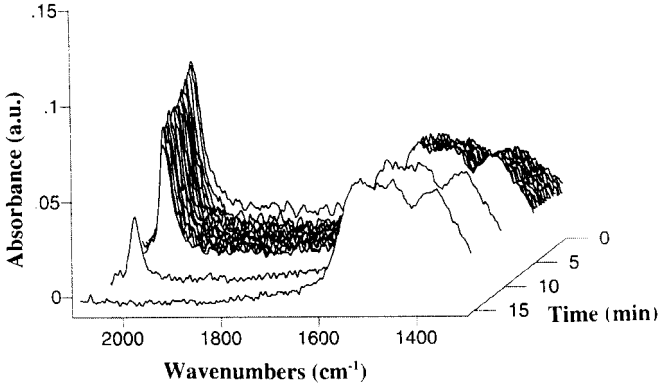

FIG. 8. Time resolved IR spectra during CO_2 adsorption on Pt/ZrO_2, $T = 775$ K, $pCO_2 = 0.25$, total flow 30 ml $\cdot$ min^{-1}.

that the importance of carbonate, for CO_2/CH_4 reforming, was previously suggested by Nakamura *et al.* (13). They reported that the activity of a Rh/SiO_2 catalyst which did not form carbonates was enhanced by adding MgO, Al_2O_3, or TiO_2, i.e., compounds which facilitate carbonate formation. Figure 8 shows that during prolonged exposure of Pt/ZrO_2 to CO_2 the band characteristic for adsorbed CO disappeared. This is explained in the following way; the carbonate formed on the support boundary decomposed on the metal to CO and adsorbed oxygen. The CO desorbs, whereas the adsorbed oxygen covers the Pt boundary making it inactive for further carbonate decomposition. When the oxygen atom is scavenged by methane the sites become available again for reaction. Based on the above results we propose a bifunctional mechanism for reforming. CO_2 is activated on the support, whereas methane is activated on the metal. The two activated species may react with each other on the Pt-ZrO_2 boundary.

Although Pt/ZrO_2 is an active catalyst for CO_2/CH_4 reforming care has to be taken during the preparation of the catalyst to ensure a large Pt-ZrO_2 boundary. When the catalyst precursor (after impregnation of the support) is calcined at 1125 K the activity of the catalyst decreased compared to a catalyst calcined at 925 K (Table 3). The increase in calcination temperature decreased the hydrogen chemisorption capacity of the catalyst. The Pt–Pt coordination number as calculated from EXAFS also increased with increasing the calcination temperature. This shows clearly that the decrease in activity was caused by sintering of the Pt particles. On the other hand, the reduction temperature does not affect the activity of Pt/ZrO_2. However, the hydrogen chemisorption capacity of this catalyst markedly decreased with increasing reduction temperature (Fig. 3, Table 4). The decrease in hydrogen chemisorption capacity is not affiliated with a decrease in activity. XAFS measurements showed that the Pt particle size is not affected by the reduction temperature (Table 4). It is clear from these results that sintering does not occur during reduction. Thus we conclude that Pt/ZrO_2 catalysts have a "strong metal

support interaction" (SMSI) which has been identified for Pt/TiO_2 catalysts (28, 29) and is also reported to occur on ZrO_2 containing catalysts (35, 36). In the SMSI state Pt is decorated by the partially reduced oxide suppressing the hydrogen chemisorption capacity, but leaving the particle size unaffected. This process can be reversed by O_2 or water. Our results showed that the SMSI state could be reverted by oxygen treatment of the sample (Table 4). During reaction conditions this SMSI state is absent, since it is possible to dissociate CO_2 on the catalyst to CO and O_{ads} as shown by IR spectroscopy (Figs. 7 + 8). The O_{ads} might be responsible for oxidizing the ZrO_x species on the Pt and, thus, minimizing the extent of decoration with oxide islands. Because the SMSI state is not present under reaction conditions, the fraction of metal exposed after low temperature reduction is representative for the Pt availability under reaction conditions.

Figure 4 shows that the H_2/CO ratio in the product stream is not one as expected from the stoichiometric reforming reaction. This is not surprising, considering that thermodynamics (Fig. 5) predicts a H_2/CO ratio of unity only at temperatures above 1150 K. This is affiliated with the reverse watergas-shift reaction (RWGS). The reaction consumes part of the H_2 produced by reforming, H_2 reacts with CO_2 to yield CO and water. Thus one finds a higher CO yield compared to H_2 and higher CO_2 conversion compared to the methane conversion. As shown in Fig. 9 the RWGS is not on thermodynamic equilibrium under our reaction conditions.

At higher temperatures (>1150 K) a H_2/CO ratio close to one can be obtained as then the water formed by the RWGS reaction can be consumed via the steam reforming (Fig. 10) to yield hydrogen and carbon monoxide. At temperatures over 1150 K the equilibrium for the steam reforming reaction shifts almost completely to the side of H_2 and CO. Thus, at these temperatures a higher driving force to produce only H_2 and CO exists.

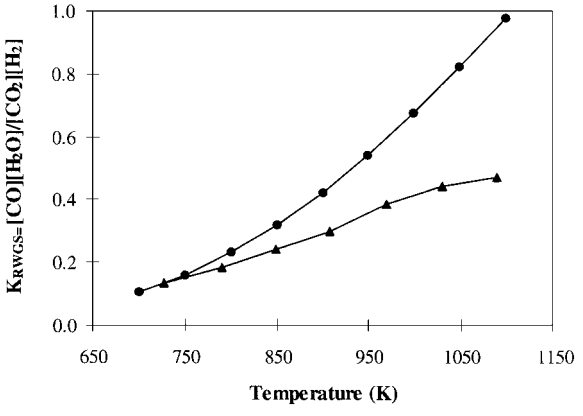

FIG. 9. Equilibrium values for the RWGS reaction ($H_2 + CO_2 \rightarrow CO + H_2O$) obtained over Pt/ZrO_2 under CO_2 reforming conditions (▲) and as calculated from thermodynamics (●).

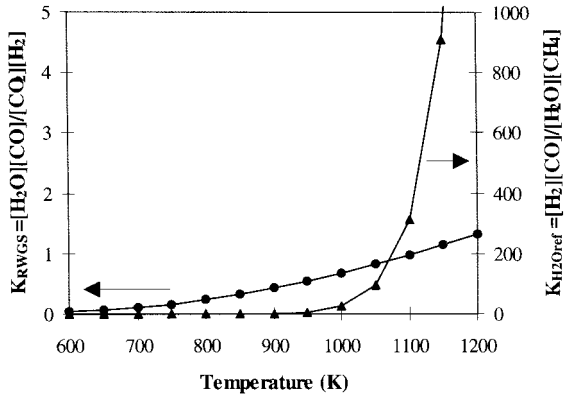

FIG. 10. *K*-values for the RWGS reaction ($H_2 + CO_2 \rightarrow CO + H_2O$) (●) and steam reforming ($H_2O + CH_4 \rightarrow 3H_2 + CO$) (▲) as calculated from thermodynamics.

CONCLUSIONS

In supported Pt catalysts not all the exposed Pt atoms contribute equally to the activity of the catalyst for CO_2/CH_4 reforming. Pt atoms on the support–metal perimeter determine the activity. This is explained in terms of the CO_2 activation via carbonate species on the support that must be in the proximity of the Pt particles to react with the methane which is activated on the Pt. The perimeter concentration can be changed by either changing the metal loading or by changing the calcination temperature. The significance of the support is also manifested in the low activity of Pt black and Pt/SiO_2 which were incapable of forming carbonates on the support and showed a low activity for reforming. During high temperature reduction SMSI states evolve on Pt/ZrO_2 catalysts. However, this state does not influence the activity of the catalyst, because adsorbed oxygen (from CO_2 dissociation) destroys it under reaction conditions.

ACKNOWLEDGMENTS

This project was supported by the EU, Joule II programme, subprogramme: Energy from fossil sources: hydrocarbons, Contract JOU2-CT92-0073. The XAFS measurements were carried out at the SRS, Daresbury Laboratory, United Kingdom. The authors are indebted to M. Englisch and A. Jentys for valuable discussions on XAFS of Pt/ZrO_2.

REFERENCES

1. Aschcroft, A. T., Cheetham, A. K., Green, M. L. H., and Vernon, P. D. F., *Nature* **225**, 352 (1991).
2. Richardson, J. T., and Paripatyadar, S. A., *Appl. Catal.* **61**, 293 (1990).
3. Seshan, K., and Lercher, J. A., *in* "Carbon Dioxide: Environmental Issues" (J. Paul and C. Pradier, Eds.), p. 16, The Royal Soc. Chem., Cambridge, 1994.
4. Bhattacharya, A., and Chang, V. W., Int. Conf. on Catalyst Deactivation, Oostende, Oct. 1994, *Stud. Surf. Sci. Catal.* **88**, 207 (1994).
5. Kurz, G., and Teuner, S., *Erdol. Kohle* **43**(5), 171 (1990).

6. van den Oosterkamp, P. F., Chen, Q., Overwater, J. A. S., Ross, J. R. H., and van Keulen, A. N. J., "Meeting of Large Chemical Plants, Antwerp, Belgium, Oct. 1995."
7. Bodrov, I. M., and Apel'baum, L. O., *Kinet. Katal.* **8**, 379 (1967).
8. Udengaard, N. R., Bak Hansen, J. H., Hanson, D. C., and Stal, J. A., *Oil Gas J.* **90**, 62 (1992).
9. Fischer, F., and Tropsch, H., *Brennst. Chem*. 39 (1928).
10. Solymosi, F., Kutsan, Gy., and Erdohelyi, A., *Catal. Lett.* **11**, 149 (1991).
11. Vernon, P. D. F., Green, M. L. H., Cheetham, A. K., and Ascroft, A. T., *Catal. Today* **13**, 417 (1992).
12. Qin, D., and Lapszewicz, J., *Catal. Today* **21**, 551 (1994).
13. Nakamura, J., Aikawa, K., Sato, K., and Uchijima, T., *Catal. Lett.* **25**, 265 (1994).
14. Rostrup Nielsen, J. R., *J. Catal.* **144**, 38 (1993).
15. Perera, J. S., Sankar, J. W., and Thomas, J. M., *Catal. Lett.* **11**, 219 (1991).
16. Tsipouriari, V. A., Efstathiou, A. M., Zhang, Z. L., and Verykios, X. E., *Catal. Today* **21**, 579 (1994).
17. Mark, M. F., and Maier, W. F., *Angew. Chem. Int. Ed. Engl.* **15-16**, 33 (1994).
18. Sakai, Y., Saito, H., Sodesawa, T., and Nozaki, F., *React. Kinet. Catal. Lett.* **24**, 253 (1984).
19. Gadalla, A. M., and Sommer, M. E., *Chem. Eng. Sci.* **44**, 2825 (1989).
20. Seshan, K., ten Barge, H. W., Hally, W., van Keulen, A. N. J., and Ross, J. R. H., *Stud. Surf. Sci. Catal.* **81**, 285 (1994).
21. Bitter, J. H., Hally, W., Seshan, K., van Ommen, J. G., and Lercher, J. A., *Catal. Today* **29**, 349 (1996).
22. Lercher, J. A., Bitter, J. H., Hally, W., Niessen, W., and Seshan, K., *Stud. Surf. Sci. Catal.* **101**, 463 (1996).
23. Seshan, K., Mercera, P. D. L., Xue, E., and Ross, J. R. H., German Patent P4313673, 1994. [International patent WO94/224042, 1994]
24. Kip, B. J., Duivenvoorden, F. B. M., Koningsberger, D. C., and Prins, R., *J. Catal.* **105**, 26 (1987).
25. Vaarkamp, M., Grondelle, J. V., Miller, J. T., Sajkowski, D. J., Modica, F. S., Lane, G. S., Gates, B. C., and Koningsberger, D. C., *Catal. Lett.* **6**, 369 (1990).
26. Paal, Z., Zhan, Z., Fulop, E., and Tesche, B., *J. Catal.* **156**, 19 (1995).
27. Scholten, J. J. F., Pijpers, A. P., and Hustings, A. M. L., *Catal. Rev.-Sci. Eng.* 27 (1985).
28. Tauster, S. J., Fung, S. C., and Garten, R. L., *J. Am. Chem. Soc.* **100**, 170 (1978).
29. Tauster, S. J., *Acc. Chem. Res.* **20**, 389 (1987).
30. Levin, M. E., Salmeron, M., Bell, A. T., and Somorjai, G. A., *J. Chem. Soc. Faraday Trans. 1* **83**, 2061 (1987).
31. Levin, M. E., Salmeron, M., Bell, A. T., and Somorjai, G. A., *J. Catal.* **106**, 401 (1987).
32. Boffa, A. B., Lin, C., Bell, A. T., and Somorjai, G. A., *Catal. Lett.* **27**, 243 (1994).
33. Koerts, T., Welters, W. J. J., and van Santen, R. A., *J. Catal.* **134**, 1 (1992).
34. Grenoble, D. C., Edstadt, M. M., and Ollis, D. F., *J. Catal.* **67**, 90 (1981).
35. Turlier, P., and Martin, G. A., *React. Kinet. Catal. Lett.* **21**, 287 (1982).
36. Dall'Agnol, C., Gervasini, A., Morazzoni, F., Pinna, F., Stukul, G., and Zanderighi, L., *J. Catal.* **96**, 106 (1985).